

Study of bursting events and effect of hole-size on turbulent bursts triggered by the fluid and mid-channel bar interaction

Md. Amir Khan and Nayan Sharma

ABSTRACT

Turbulent structures of flow around the mid-channel braid bar have not been adequately investigated so far. Of late, the intrinsic fluvial hydraulics associated with the formation of braided rivers interspersed with sand bars have been vital topics of research. In this paper, the findings yielded from a research foray on the aforementioned underlying processes are presented. For obtaining the requisite experimental data, the three-dimensional flow velocity components are measured with the help of acoustic Doppler velocimetry (ADV) and these velocity data are analyzed using quadrant bursting techniques. The flow characteristics are greatly affected by the presence of a mid-channel bar. The depth-averaged contours of turbulent parameters are analyzed in the present study. Herein, the hole size concept is adopted for separating the bursting events. The effect of hole size on the quadrant events is also studied. The experiments are performed for different submergence ratios. A new parameter, Bursting Index (BI), is proposed in this research to reflect a quantitative measure of the turbulent bursting effect on streambed elevation changes. The parameter BI is the ratio of the odd event occurrence probability to the even event occurrence probability. The high values of correlation coefficients signify that the BI is profoundly influenced by streambed elevation changes, which makes it an ideal parameter for analyzing scour and deposition phenomena in real-life water management projects. The prime focus on performing the experiments has been to analyze the impact of bar height on flow structure in the vicinity of the mid-channel bar.

Key words | acoustic Doppler velocimetry, bursting events, hole size, mid-channel bar, occurrence probability

HIGHLIGHTS

- A new parameter of Bursting Index (BI) is utilized in this research to reflect a quantitative measure of the turbulent bursting effect on streambed elevation changes.
- The high values of correlation coefficients signify that the BI is profoundly influenced by the streambed elevation changes which makes it an ideal parameter for analyzing scour and deposition phenomena in real-life water management projects.
- The prime focus on performing the experiments has been to analyze the impact of bar height on the flow structure in the vicinity of the mid-channel bar.

INTRODUCTION

In spite of the research significance of mid-channel bars, only a few studies have been reported on the underlying fluvial hydraulics in the vicinity of a mid-channel bar. The concept

of turbulent burst and its impact on near-bed stress generation was first introduced by [Kline *et al.* \(1967\)](#) as a quasi-periodic process which leads to momentum transfer in the boundary

doi: 10.2166/ws.2020.138

Md. Amir Khan (corresponding author)
Galgotias College of Engineering and Technology,
Greater Noida, 201310,
India
E-mail: amirmdamu@gmail.com

Nayan Sharma
Department of Water Resources Development and
Management,
IIT Roorkee,
Roorkee, 247667,
India

layer. Researchers such as Termini (2012) and Maity & Mazumder (2014) studied 2-D bursting events and found that the sweep event is related to the sediment entrainment. In the past few years, research on the coherent structure of turbulent flow has significantly increased and been executed both in natural channels (Nikora & Goring 2000) as well as in laboratory flumes (Detert *et al.* 2007). The flow characteristics at locations downstream and upstream of a submerged structure have been researched greatly in the past, but the flow characteristics along the sides of a submerged structure have not been much investigated (Sarkar & Ratha 2014; Shamloo & Pirzadeh 2015). In this paper, the turbulent flow characteristics along the sides of the mid-channel bar are investigated and analyzed in detail.

Mid-channel bar formation is the prime reason for initiation of the braiding process (Ashmore 1991). Researchers such as Ferguson (1993) and Ashworth (1996) have observed that the slight change in competence leads to the initial deposition which further attenuates more deposition and with the lapse of time it takes the shape of island.

In the recent past, Mazumder & Ojha (2007) and other researchers also used the fixed bed form configurations for experimentally studying the interaction of these bedforms with the flow. In fact, it is difficult and impractical to analyze in a lab flume the effect of a mid-channel bar on the flow characteristics (without fixing it) by simultaneously allowing changes in the flow as well as in the bar. The focus of the present experiments is to investigate the fluvial parametric changes brought about by turbulent bursts in the vicinity of a mid-channel bar of given configuration. The present scientific study on fluvial interactions with a mid-channel bar of given configuration due to fluctuating turbulent bursts would undoubtedly lead to better understanding of the resulting internal modifications in the turbulent flow structure. Based on extensive laboratory experimentations, Sharma (2004) observed that the modeling to precisely reproduce fluvial conditions of actual prototype braided river configurations of a highly transient mid-channel bar running into kilometre dimensions (as in the case of the hugely large Brahmaputra river), which is impossible to achieve in laboratory flume experiments due to inherent limitations. To circumvent the practical difficulties of modelling a prototype flow regime with the complex fluvial landforms of a large braided stream in a lab flume, an

idealized form of the mid-channel bar of a braided river has been adopted for the present study.

In this study, the turbulence generated in the near-bed region by the mid-channel bar is analyzed using the bursting approach. The concept of hole size has been used for removing low-intensity events from the velocity fluctuations analysis. The flow characteristics are greatly affected by the presence of a mid-channel bar. Therefore, in this study, the turbulence parameter contours are analyzed for different experimental conditions.

EXPERIMENTAL PROCEDURE

The experiments were performed in a flume 10 m long, 2.6 m wide and 1 m deep (Figure 1(a)). The experiments were performed at a discharge rate of 0.2 m³/sec. The details of the experiments are given in Table 1. The bed slope of the flume was kept constant at 0.005. The depth of water was maintained with the help of the tailgate. All experiments were carried out in clear-water conditions. The bed of the flume was prepared with sediment of uniform grading with $D_{50} = 0.25$ mm.

D_{50} is the sieve size for which 50 percent of bed material is finer. The measurement of velocity is done by using acoustic Doppler velocimetry (ADV). The specification of the ADV is given below.

Resolution	0.01 cm/s
Sampling Volume	0.09 cc
Sampling Rate	0.1–50 Hz
Distance to Sampling Volume	5 cm

The ADV utilizes the concept of Doppler shift for measuring the velocity. The shift in frequency is used for computing the flow velocity. The noise in the signal is removed by the phase threshold method (Nikora & Goring 2000). Following Nikora & Goring (2000), data having a correlation coefficient less than 70 are excluded from the velocity data. A frequency of 20 Hz is used in the present study for velocity measurements as per Voulgaris & Trowbridge (1998).

The experiments were performed for three different submergence ratios (Table 1). Submergence ratio is the ratio of

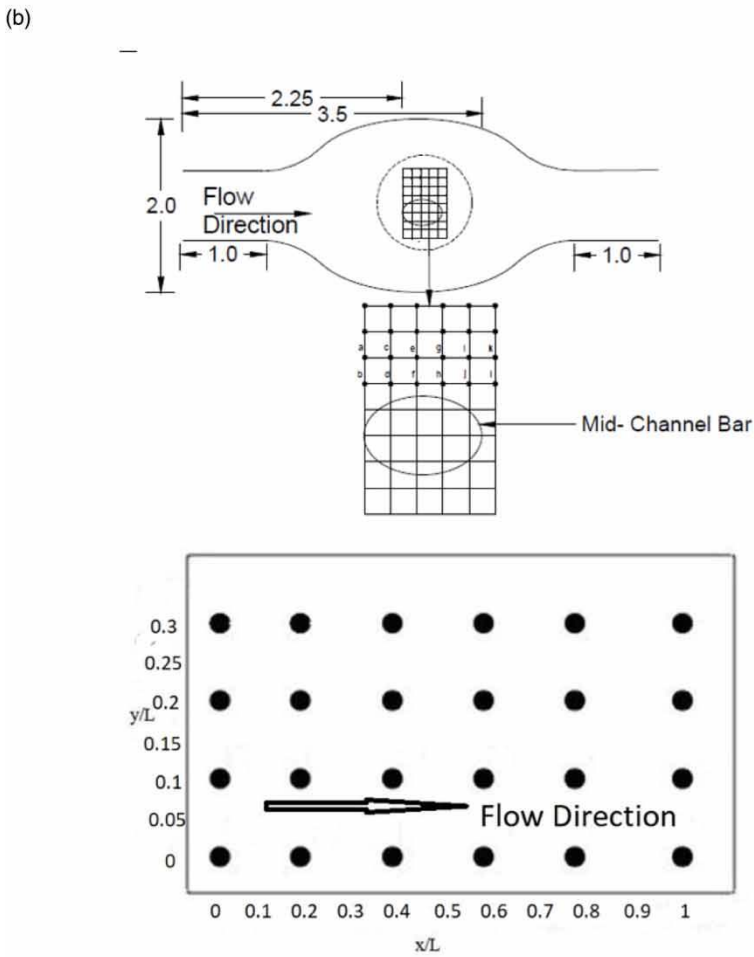


Figure 1 | (a) The model of braided bar constructed in a River Engineering Lab IIT Roorkee; (b) the sketch of the mid-channel bar model and measuring points (all dimensions in metres).

Table 1 | Details of experiments

Experimental run	Depth of flow (cm)	Bar size ($L \times B \times H_b$)	Discharge cm^3/sec	Submergence ratio
1R	28	100 by 75 by 8 cm	200,000	0.28
2R	28	100 by 75 by 8 cm	200,000	0.46
3R	28	100 by 75 by 8 cm	200,000	0.61
4R	28	No bar	200,000	–

the height of mid-channel bar to the depth of flow. The experiment performed for the no-bar condition (4R) run was used as a test run for comparing with the other experimental runs. Experimental runs 1R, 2R and 3R were performed in the presence of a bar and thus, these runs have been termed as bar runs in this study. Experimental run 4R is termed the no-bar run. The gate was provided at the end of the flume for maintaining the flow depth. The flow measurements were taken after equilibrium had been reached. The bed level becomes constant after attainment of equilibrium. In Table 1, L indicates the major axis and B indicates the minor axis of the elliptical bar. The experiments are performed for clear-water conditions.

Velocity measurements were taken for 4 min duration at each point to ensure that observations could become stationary. The velocity measurements were taken at 24 points shown by the dots in Figure 1(b). The velocity measurement was taken at ten different depths for each point (Table 2). The velocity measurement was also done in the near-bed region ($z/h \leq 0.070$). Here, the depth of flow is shown by the symbol h ; z is the vertical distance of a point from the bed.

Table 2 | Shows the relative depths at which velocities are measured for each point**Relative depth (z/h)**

0.047
0.049
0.052
0.055
0.057
0.060
0.062
0.064
0.067
0.070

The measurements of bed levels were done by using the manually adjusted hook and readings were taken from the vertical movement using a scale. The complete setup of hook and scale is known as a point gauge. A Vernier scale on the point gauge had a least count of 0.1 mm.

At different points, the bed-level measurements were done before the start of the experiment and after completion of the experiment. The difference between these two levels indicated the scouring/deposition that occurred at these points. A positive value of the difference indicated deposition and a negative value signified scouring.

The wake flow characteristics in the proximity of the bar were analyzed by plotting U/u_* against the dimensionless parameter $\frac{zu_*}{\vartheta}$ (Figure 2). Here, U is mean velocity of flow, u_* is shear velocity of approaching flow, ϑ is dynamic viscosity of water and z is vertical distance from the bed. In Figure 2, the straight line follows the Prandtl–Karman log-law distribution as shown by Equation (1):

$$\frac{U}{u_*} = \frac{1}{k} \ln\left(\frac{z}{y_0}\right) \quad (1)$$

Here, k is the von Karman constant and its value is 0.41 for clear water, and y_0 is zero velocity level.

The expression for y_0 is given by Equation (2) (van Rijn 1993):

$$y_0 = \frac{\vartheta}{9.1u_*} \quad (2)$$

The velocity profiles closely followed the log-law line. This indicated that the flow is uniform in the proximity of the bar.

The errors in velocity measurements have been computed for different velocity ranges as shown below.

Nominal velocity range (cm/sec)	ADV velocity error (mm/sec)
±5	±0.92
±10	±0.98
±20	±1.22
±30	±1.89

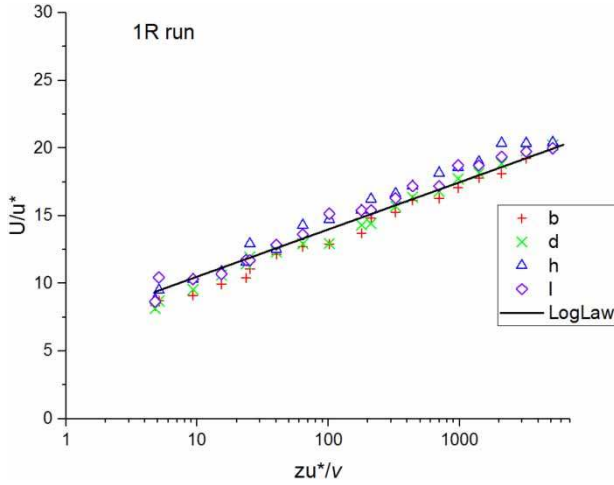


Figure 2 | The variations of U/u_* versus $\frac{zu_*}{v}$ for four different points located in the vicinity of the mid-channel bar.

TWO-DIMENSIONAL QUADRANT ANALYSIS

The conventional quadrant method involves studying the relationship between fluctuations of velocity components u' and w' . Nezu *et al.* (1994) observed that the strong events were only responsible for Reynolds stress. Mazumder & Ojha (2007), Ojha & Mazumder (2010), Duan *et al.* (2011) and Maity & Mazumder (2014) observed that the low-intensity events have much less contribution to the turbulent burst. Therefore, the concept of hole size has been used for removing the low-intensity events from the velocity fluctuations analysis. As the hole size increases, the velocity fluctuations of lesser magnitude are removed. In other words, the increase in hole size leads to the retainment of only strong events. Due to the significance of the hole size concept, the effect of it on the turbulence generated by the bar is analyzed.

The arbitrary hole size is defined by Equation (3):

$$|u'w'| = H\sqrt{u'^2}\sqrt{w'^2} \tag{3}$$

Here, H indicates the hole size, the over-bar indicates the time averaged value, u' and w' indicate the instantaneous fluctuations in longitudinal and vertical turbulent direction respectively, and $\sqrt{u'^2}$ and $\sqrt{w'^2}$ represent the root mean square values of longitudinal and vertical fluctuation respectively.

Events for which their fluctuating velocity product is less than H times the product of their root mean square values are termed weak events.

For weak events,

$$|u'w'| < H\sqrt{u'^2}\sqrt{w'^2}$$

Events for which their fluctuating velocity product is greater than or equal to H times the product of their root mean square values are termed strong events.

For strong events $|u'w'| \geq H\sqrt{u'^2}\sqrt{w'^2}$ instantaneous Reynolds stress has been filtered by applying the function $I_{i,H}[u', w']$ where $i = I, II, III, IV$ shows the quadrant of the event and H represents the hole size.

The total Reynolds stress contribution from i quadrant after removing the hole region H is given by Equation (4):

$$\langle u'w' \rangle_{i,H} = \frac{1}{n} \int_0^n u'(t)w'(t)I_{i,H}[u', w']dt \tag{4}$$

The discriminating function $I_{i,H}[u', w']$ is defined below (Maity & Mazumder 2014):

$$I_{i,H}[u', w'] = 1, \text{ if } (u', w') \text{ is in the } i \text{ Quadrant and if } u'w' \geq H[u_{\text{rms}}w_{\text{rms}}]$$

$$I_{i,H}[u', w'] = 0, \text{ otherwise} \tag{5}$$

The function $I_{i,H}[u', w']$ shown in Equation (5) was used for removing the events that lay in the hole region. Hole sizes of 1 and 1.5 were used in this research as per Mazumder & Ojha (2007).

Occurrence probability contours of bursting events

Bursting events play an important role in understanding turbulent flow structure (Duan *et al.* 2011). In this section, the effect of the mid-channel bar on near-bed turbulence structure is investigated using the quadrant technique.

Quadrant analysis of bursting events indicates that the sweep events are linked with the high-velocity fluid moving away from the main flow into the boundary layer (Salim *et al.* 2017). Ejection events represent the low velocity fluid moving into the main flow away from the boundary

layer. The sweep events create many small-scale eddies in the boundary layer (Cellino & Lemmin 2004). Outward interaction events create high-velocity pulses moving toward the main flow from the boundary layer and in the flow direction, while inward interaction events create low-velocity pulses moving away from the outer flow region into the boundary layer and opposite to the direction of flow (Cuthbertson & Ervine 2007).

The occurrence probability of each quadrant event is calculated by Equation (6) (Termini & Sammartano 2008):

$$f_k(z) = \frac{\sum_{t=0}^T E_k(z, t)}{\sum_{t=0}^T E_I(z, t) + \sum_{t=0}^T E_{II}(z, t) + \sum_{t=0}^T E_{III}(z, t) + \sum_{t=0}^T E_{IV}(z, t)} \quad (6)$$

Here $\sum_{t=0}^T E_k(z, t)$ is the number of events that belong to the k -th quadrant after removing the events within the hole, and T is the length of measurement time.

The measurement points are elaborated in Figure 1(b). The upstream end of the bar is considered as the origin. The length of the mid-channel bar (L) is used for normalizing the longitudinal (x) and transverse distance (y).

Figures 3 and 4 show the depth-averaged contours of quadrant event occurrence probability for hole size of 0 and 1.5 respectively (1R experimental run). Zero hole size means that all events are considered for burst analysis. The x -axis of these figures shows the normalized longitudinal distance and y -axis displays the normalized transverse distance.

Results indicate that even events are dominant at the upstream region ($x/L = 0$) and odd events are dominant at the downstream region of the bar ($x/L = 1$). By observing the contours, it was observed that the maximum values of sweep and ejection event occurrence probability are 0.3 and 0.32 respectively for zero hole size (Figure 3). The maximum value of sweep and ejection event occurrence probability increases to 0.34 and 0.37 respectively for 1.5 hole size (Figure 4). Similarly, the maximum values of

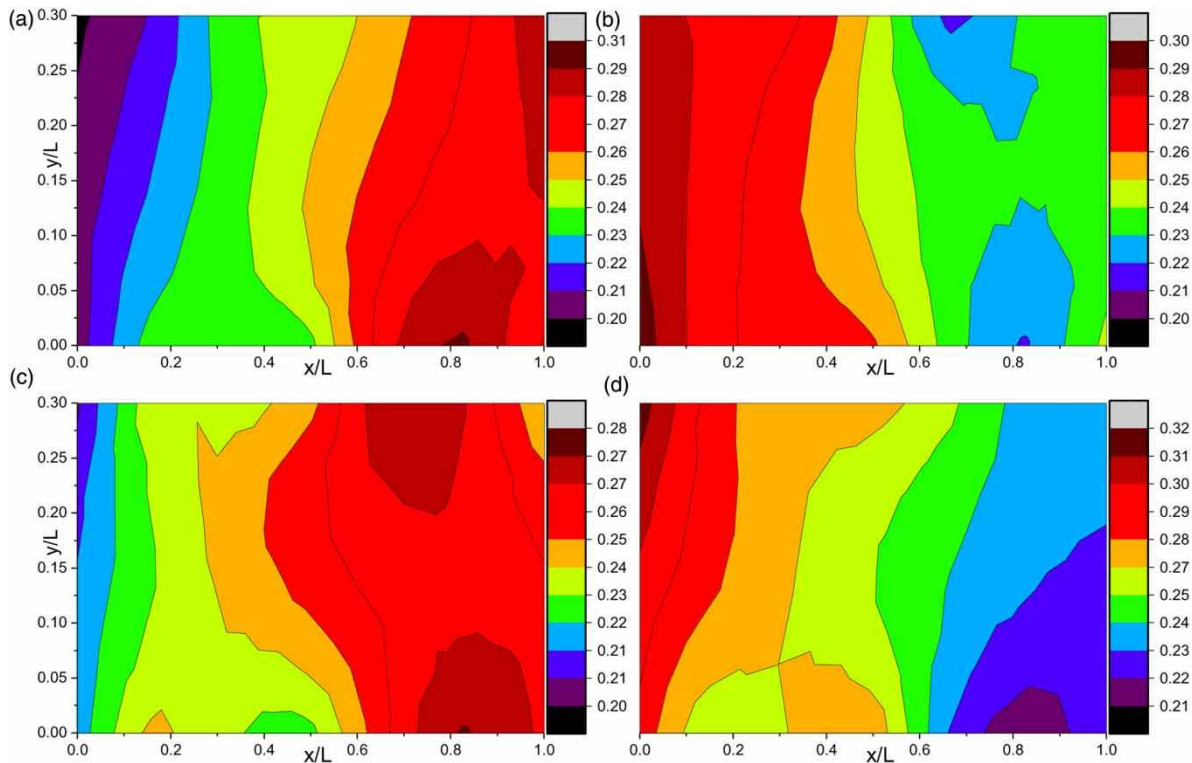


Figure 3 | (a)–(d) The depth-averaged occurrence probability contours of outward interaction, ejection, inward interaction and sweep event respectively for zero hole size (1R experimental run).

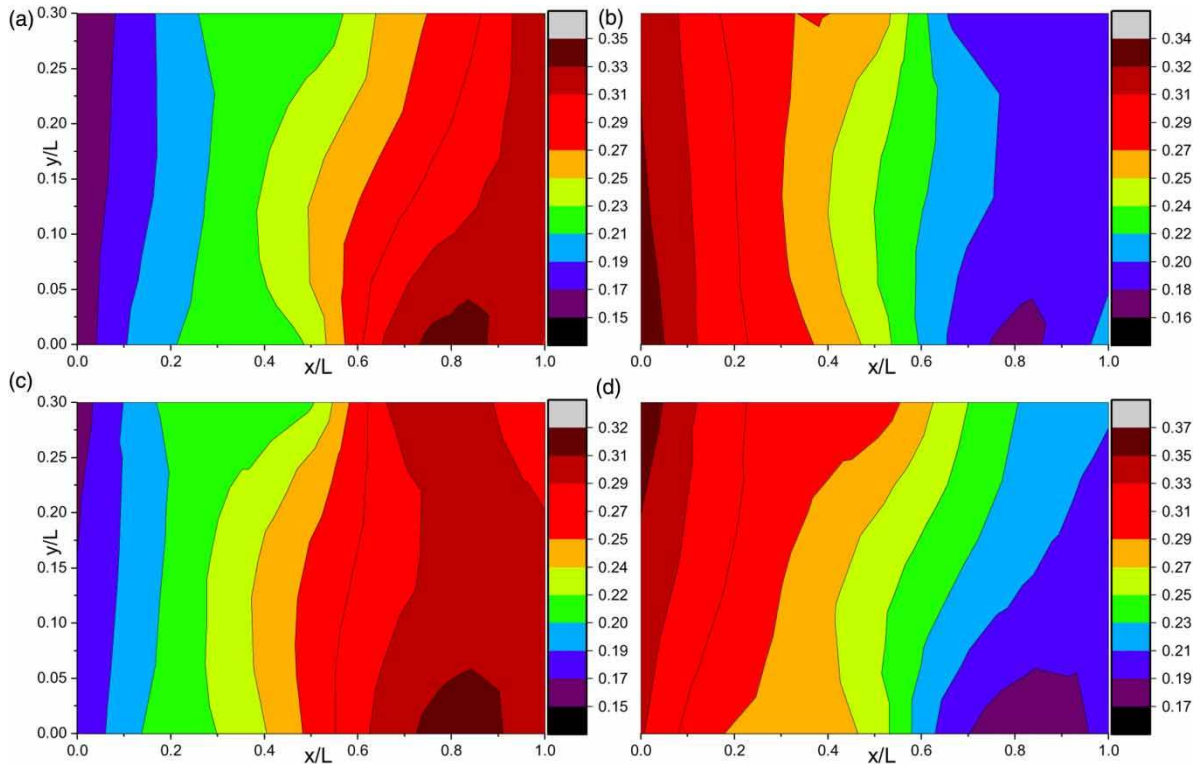


Figure 4 | (a)–(d) The depth-averaged occurrence probability contours of outward interaction, ejection, inward interaction and sweep event respectively for 1.5 hole size (1R experimental run).

occurrence probability of inward and outward interaction events increase with increase in the hole size. The above discussion indicates that the magnitude of occurrence probability of highly probable quadrant events increases with increase in the hole size. The results are in accordance with Mazumder & Ojha (2007), Izadinia *et al.* (2013) and Maity & Mazumder (2014).

Figure 5 shows the depth-averaged occurrence probability contours for the no-bar run at zero hole size (4R experimental run). By observing Figure 5, it is found that the sweep and ejection events have higher occurrence probability throughout the region of contours with the values lying between 0.23 and 0.35. The occurrence probabilities of inward and outward interaction events have low values ranging from 0.14 to 0.24. The above discussions indicate that the even events are dominant throughout the whole region for the no-bar run and the occurrence probability of highly probable events further increases with increase in the hole size.

While comparing the no-bar run contour (Figure 5) with the bar run contour (Figure 3), it can be observed that for the no-bar run the contours are fairly uniform. Bar run contours

(Figures 3 and 4) are highly non-uniform in nature, while the even events have high probability near the upstream region and have low probability at regions downstream of the bar. The zone of highly probable odd events lies at the downstream region of the bar ($x/L = 1$).

Figures 3 and 6 show the depth-averaged occurrence probability contours for experimental runs 1R and 3R respectively (zero hole size). Figure 7(a)–7(c) shows the Dimensionless bed-level contours for experimental runs 1R, 2R and 3R respectively. Scouring/deposition is normalized by the depth of flow.

From Figure 7 it is observed that the scouring occurs for regions for which x/L lie between (0 to 0.6) and deposition occurs for regions ($0.6 > x/L < 1$). From Figure 7, it is also observed that the maximum magnitude of dimensionless scouring for the 1R experimental run is 0.07. The magnitude of dimensionless scouring increases to 0.11 for the 3R experimental run. While referring to Figure 7, it can be further observed that the maximum value of dimensionless deposition is 0.14 for the 1R experimental run and it increases to 0.17 for the 3R experimental run.

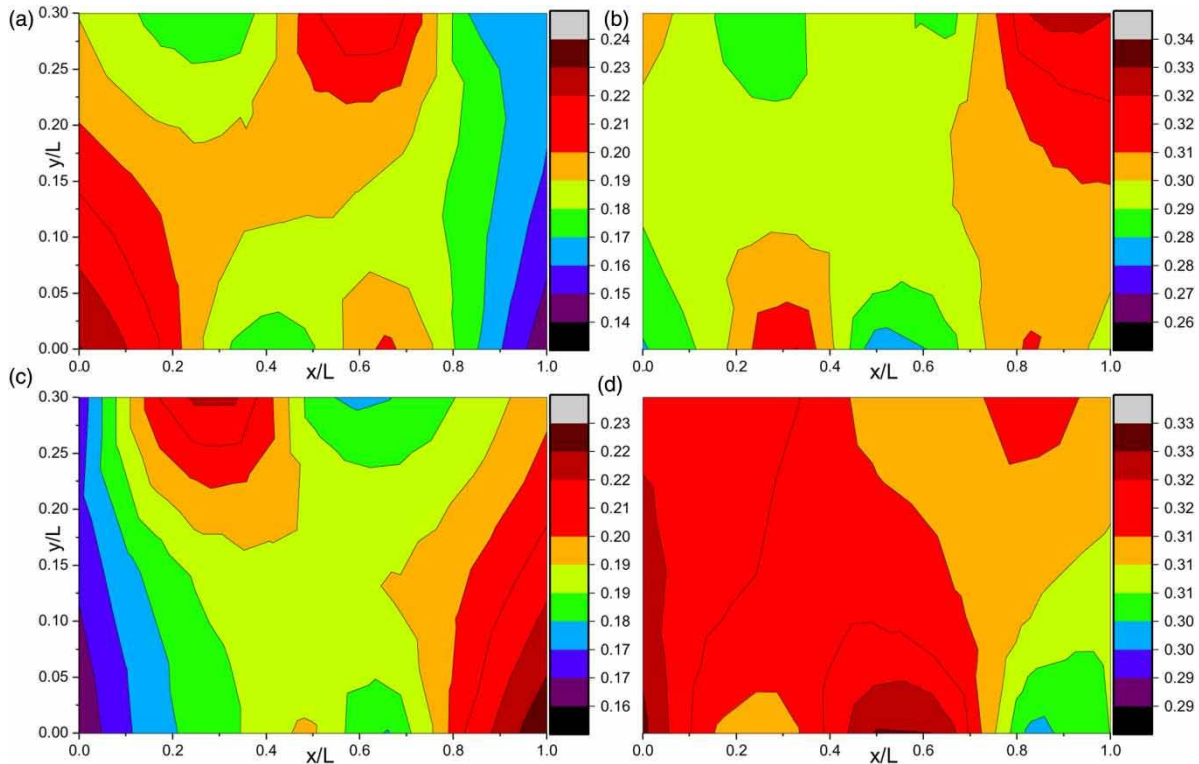


Figure 5 | (a)–(d) The depth-averaged occurrence probability contours of outward interaction, ejection, inward interaction and sweep event respectively for zero hole size (4R experimental run).

While comparing Figures 3 and 7(a), it can be discerned that the dominance of sweep and ejection events at the scouring area and interaction events are governing the depositional area. Similar results are observed by comparing Figure 6 with Figure 7(c) respectively.

The above discussion brings out that the even events are main contributors to the extreme turbulent burst at the region of scouring and interaction events are major contributors to the turbulent burst in the depositional region. These results are in accordance with Khan *et al.* (2017).

Khan (2018) has defined the parameter of Bursting Index for analyzing the flow structure. The Bursting Index (BI) is the ratio of the summation of odd events to the summation of even events (Equation (7)). The main significance of the BI parameter is that it takes into account the effect of all quadrant events.

$$BI = \frac{f_1 + f_3}{f_2 + f_4} \quad (7)$$

Figure 8(a) depicts the variation of BI with the scouring/deposition that occurred for the 1R experimental run.

Figure 8(a) shows that the BI exhibits a linear relationship with the scouring/deposition phenomenon observed with coefficient of determination R^2 and Pearson R value equal to 0.90 and 0.95 respectively. Similar results are observed from the BI plots for the 2R and 3R experimental runs (Figure 8(b) and 8(c)). The high values of correlation coefficients indicate that the BI is directly linked with the bed elevation changes that occurred.

RESULTS AND DISCUSSION

Results show that the even events are dominant at the upstream end region ($x/L = 0$), and odd events are dominant at the downstream end of the bar ($x/L = 1$).

Researchers have observed that the strong events have been primarily responsible only for Reynolds stress. Researchers have also observed that the low-intensity events have much less contribution to the turbulent burst. Therefore, the concept of hole size has been used for removing the low-intensity events from the velocity fluctuations

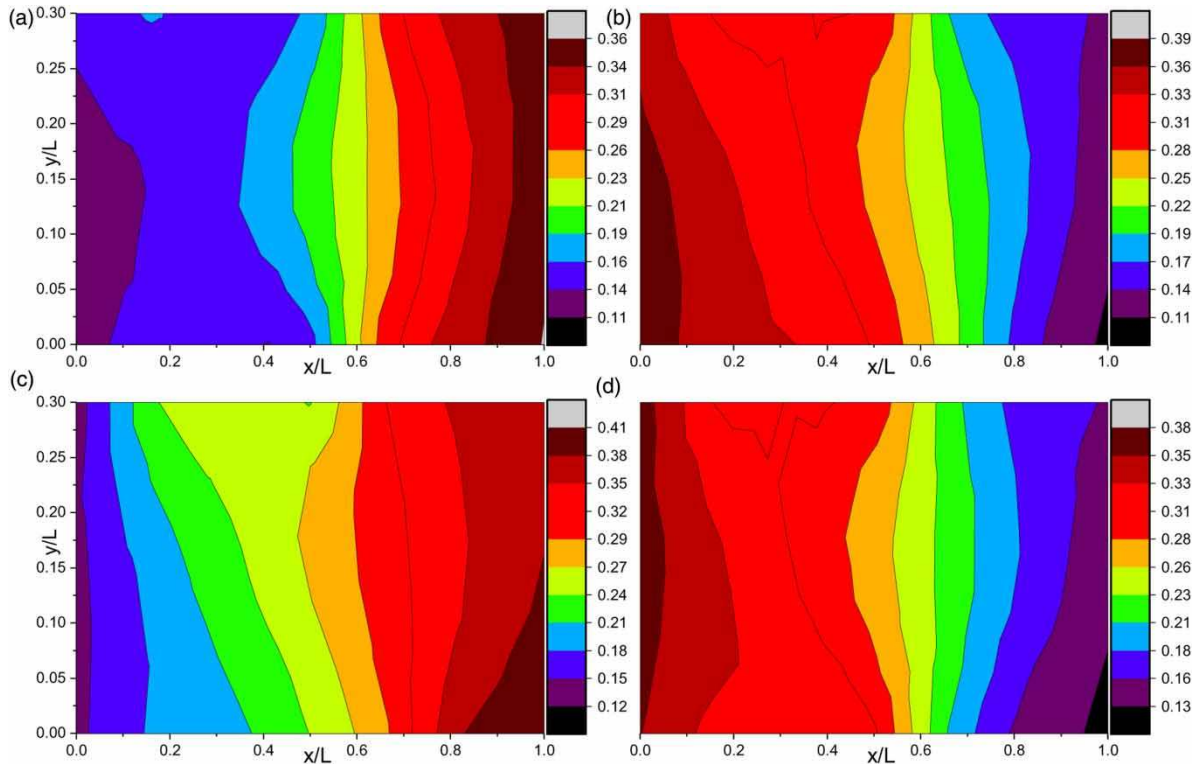


Figure 6 | (a)–(d) The depth-averaged occurrence probability contours of outward interaction, ejection, inward interaction and sweep event respectively for zero hole size (3R experimental run).

analysis. As the hole size increases, velocity fluctuations of lesser intensities are removed. In other words, the increase in hole size leads to the retainment of only strong-intensity events. Due to the significance of the hole size concept, the effect of it on the turbulence generated by the bar is analyzed.

For an area located close to the upstream end of the bar, the maximum value of sweep and ejection event occurrence probability increases as the hole size increases. At a region located near the downstream end of the bar, the maximum values of occurrence probability of inward and outward interaction events show an increasing trend with the size of the hole.

These above results show that the magnitude of occurrence probability of highly probable quadrant events further increases with increase in the hole size. This indicates that the strong events are mostly present in the dominant quadrant.

For the no-bar condition, the even events are dominant throughout the contour. But for bar conditions, the region of high-magnitude even events is separated from the high-magnitude odd events.

The results indicate that the presence of a bar leads to the creation of two regions: (1) near-upstream end of the bar and (2) near-downstream end of the bar. The even events dominate in the first region and the odd events dominate in the second region.

The results further indicate that the magnitude of scour in the scouring region increases as the submergence ratio increases. The magnitude of deposition in the depositional region also registers increment with increase in the submergence ratio. In other words, the increase in height of the bar causes more scouring near the upstream end of the bar and more deposition near the downstream of the bar. Since these experiments were performed in clear-water conditions, the above observations indicate that the sediments scoured at the upstream region get deposited at the region close to the downstream end of the bar.

The new parameter of BI is proposed in this study to reflect a quantitative measure of the turbulent bursting effect on the streambed elevation changes observed in the proximity of the bar. The main significance of the BI parameter is that it takes into account the combined effect of all quadrant events

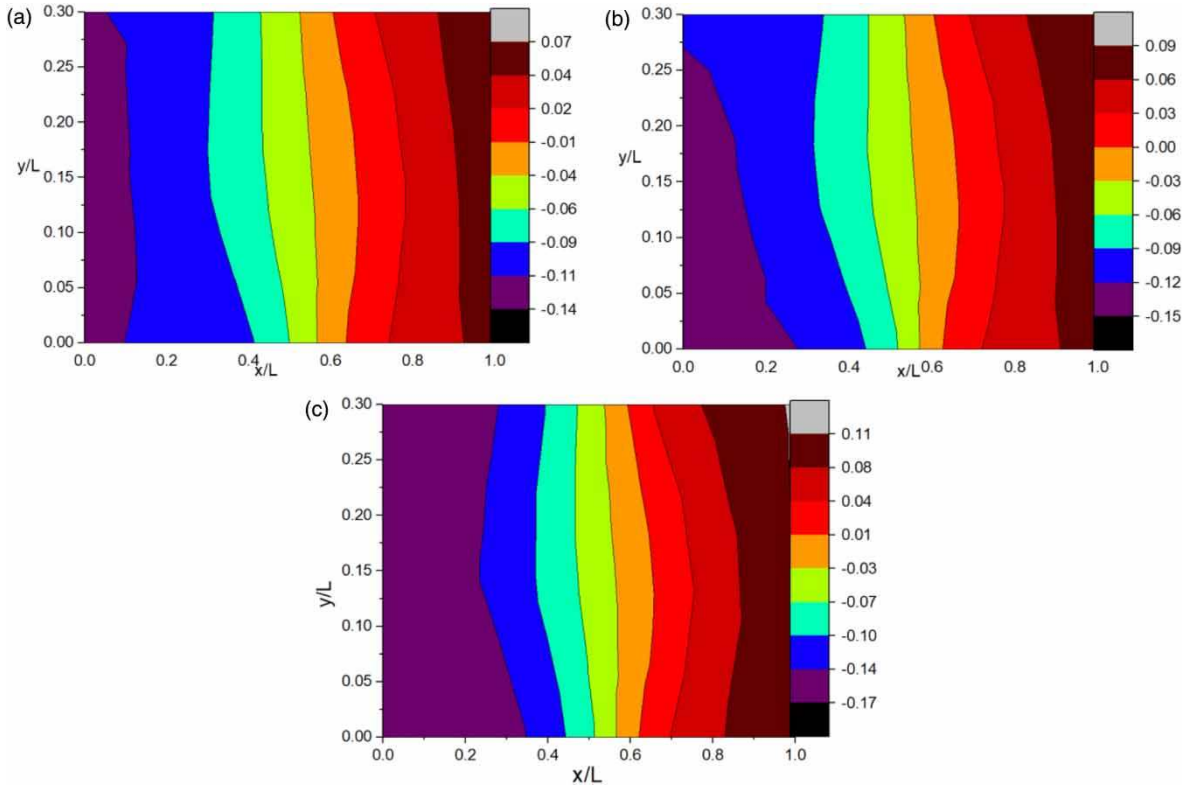


Figure 7 | (a)–(c) The contours of dimensionless scouring/deposition that occurred in the vicinity of the mid-channel bar for 1R, 2R and 3R experimental run respectively.

in the fluvial process. The result shows that the BI exhibits a linear relationship with the scouring/deposition phenomenon observed with a correlation coefficient greater than 0.9 for all experimental runs. The high values of correlation coefficients signify that the BI is profoundly influenced by the streambed elevation changes, which makes it an ideal parameter for analyzing scour and deposition phenomena in real-life water management projects.

CONCLUSIONS

The following major conclusions have been yielded from the analysis of experimental data in the present study as summarized below:

1. For bar runs, the even events are dominant in the upstream region of the bar ($x/L = 0$) and the odd events are dominant in regions located near the downstream end of the mid-channel bar ($x/L = 1$).
2. While analyzing the no-bar experimental run contours with respect to the bar run contours, it is observed that

for the no-bar run the contours are fairly uniform. In contrast, bar run contours are highly non-uniform in nature. The bar presence causes discernible non-uniformity in the coherent structure of turbulent flow.

3. Analysis of the bed-level contours has brought out that the magnitude of scour at the scouring region increases as the submergence ratio increases. The magnitude of deposition at the depositional region also increases with increase in the submergence ratio. In other words, the increase in the height of the bar causes more scouring near the upstream region and more deposition in the downstream region of the bar.
4. The results indicate that the sweep and ejection events are dominant in the region of scouring. In a similar manner, the inward and outward interaction events are dominant in the region of deposition. This occurrence highlights that the even events are major contributors to the extreme turbulent burst in the region of scouring, while the odd events are major contributors to the turbulent burst in the depositional region.

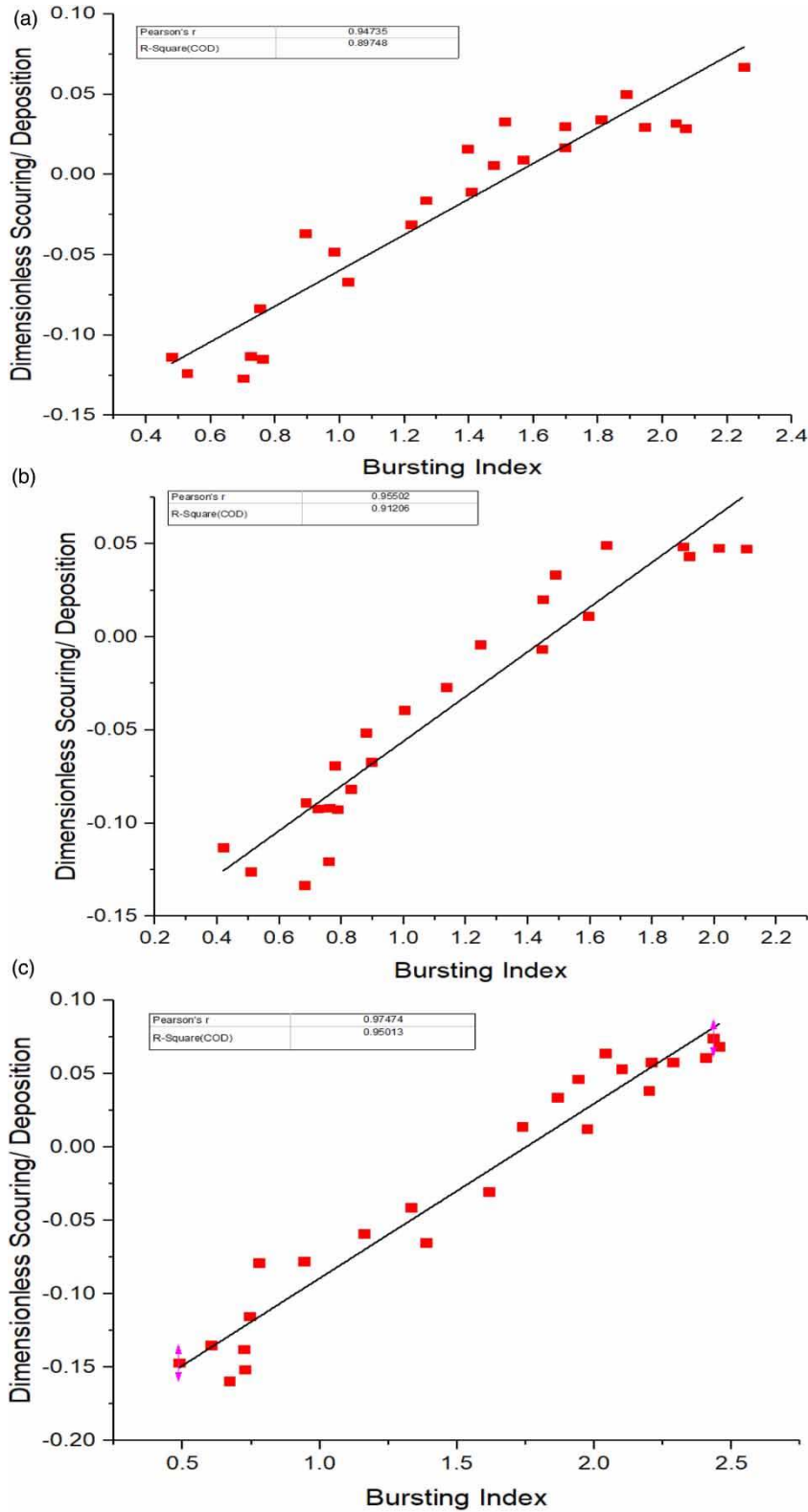


Figure 8 | (a)–(c) The variation of Bursting Index with the magnitude of dimensionless scouring/deposition that occurred in the vicinity of the mid-channel bar for the 1R, 2R and 3R experimental runs respectively.

5. A new parameter of Bursting Index is proposed in this research to reflect a quantitative measure of the turbulent bursting effect on the streambed elevation changes. The BI parameter shows linear relationships with the scouring/deposition processes that occur in the proximity of the bar with coefficient of determination R^2 and Pearson R values above 0.9 for all runs with a bar. The high values of correlation coefficients signify that the BI is profoundly influenced by the streambed elevation changes, which makes it an ideal parameter for analyzing scour and deposition phenomena in real-life water management projects.

DATA AVAILABILITY STATEMENT

All relevant data are included in the paper or its Supplementary Information.

REFERENCES

- Ashmore, P. E. 1991 [How do gravel-bed rivers braid?](#) *Canadian Journal of Earth Sciences* **28** (3), 326–341.
- Ashworth, P. J. 1996 [Mid-channel bar growth and its relationship to local flow strength and direction.](#) *Earth Surface Processes and Landforms* **21** (2), 103–123.
- Cellino, M. & Lemmin, U. 2004 [Influence of coherent flow structures on the dynamics of suspended sediment transport in open-channel flow.](#) *Journal of Hydraulic Engineering* **130** (11), 1077–1088.
- Cuthbertson, A. J. & Irvine, D. A. 2007 [Experimental study of fine sand particle settling in turbulent open channel flows over rough porous beds.](#) *Journal of Hydraulic Engineering* **133** (8), 905–916.
- Detert, M., Weitbrecht, V. & Jirka, G. H. 2007 Simultaneous velocity and pressure measurements using PIV and multi layer pressure sensor arrays in gravel bed flows. In: *HMEM 2007*, Lake Placid, NY, USA.
- Duan, H., He, L., Wang, G. & Fu, X. 2011 [Turbulent burst around experimental spur dike.](#) *International Journal of Sediment Research* **26** (4), 471–486, 523.
- Ferguson, R. I. 1993 [Understanding braiding processes in gravel-bed rivers: progress and unsolved problems.](#) *Geological Society, London, Special Publications* **75** (1), 73–87.
- Izadinia, E., Heidarpour, M. & Schleiss, A. J. 2013 [Investigation of turbulence flow and sediment entrainment around a bridge pier.](#) *Stochastic Environmental Research and Risk Assessment* **27** (6), 1303–1314.
- Khan, M. A. 2018 [Experimental Study on Turbulence in the Vicinity of Mid-Channel Bar of Braided River Reach.](#) Doctoral thesis, IIT Roorkee, Roorkee, India.
- Khan, M. A., Sharma, N. & Singhal, G. D. 2017 [Experimental study on bursting events around a bar in physical model of a braided channel.](#) *ISH Journal of Hydraulic Engineering* **23** (1), 63–70.
- Kline, S. J., Reynolds, W. C., Schraub, F. A. & Runstadler, P. W. 1967 [The structure of turbulent boundary layers.](#) *Journal of Fluid Mechanics* **30** (4), 741–773.
- Maity, H. & Mazumder, B. S. 2014 [Experimental investigation of the impacts of coherent flow structures upon turbulence properties in regions of crescentic scour.](#) *Earth Surface Processes and Landforms* **39** (8), 995–1013.
- Mazumder, B. S. & Ojha, S. P. 2007 [Turbulence statistics of flow due to wave–current interaction.](#) *Flow Measurement and Instrumentation* **18** (3–4), 129–138.
- Nezu, I., Nakagawa, H. & Jirka, G. H. 1994 [Turbulence in open-channel flows.](#) *Journal of Hydraulic Engineering* **120** (10), 1235–1237.
- Nikora, V. & Goring, D. 2000 [Flow turbulence over fixed and weakly mobile gravel beds.](#) *Journal of Hydraulic Engineering* **126** (9), 679–690.
- Ojha, S. P. & Mazumder, B. S. 2010 [Turbulence characteristics of flow over a series of 2-D bed forms in the presence of surface waves.](#) *Journal of Geophysical Research: Earth Surface* **115** (F4), F04016.
- Salim, S., Pattiaratchi, C., Tinoco, R., Coco, G., Hetzel, Y., Wijeratne, S. & Jayaratne, R. 2017 [The influence of turbulent bursting on sediment resuspension under unidirectional currents.](#) *Earth Surface Dynamics* **5** (3), 399–415.
- Sarkar, A. & Ratha, D. 2014 [Flow around submerged structures subjected to shallow submergence over plane bed.](#) *Journal of Fluids and Structures* **44**, 166–181.
- Shamloo, H. & Pirzadeh, B. 2015 [Analysis of roughness density and flow submergence effects on turbulence flow characteristics in open channels using a large eddy simulation.](#) *Applied Mathematical Modelling* **39** (3–4), 1074–1086.
- Sharma, N. 2004 [Mathematical modelling and braid indicators.](#) In: *The Brahmaputra Basin Water Resources* (V. P. Singh, N. Sharma & C. S. P. Ojha, eds), Springer, Dordrecht, The Netherlands, pp. 229–260.
- Termini, D. 2012 [Turbulence structure and coherent motion in a straight laboratory flume.](#) In: *6th International Congress on Environmental Modelling and Software*, Leipzig, Germany.
- Termini, D. & Sammartano, V. 2008 [Experimental analysis of relations between coherent turbulent structures and formation of bedforms.](#) *Archives of Hydro-Engineering and Environmental Mechanics* **55** (3–4), 125–143.
- van Rijn, L. C. 1993 [Principles of Sediment Transport in Rivers, Estuaries and Coastal Seas.](#) Aqua Publications, Amsterdam, The Netherlands.
- Voulgaris, G. & Trowbridge, J. H. 1998 [Evaluation of the acoustic Doppler velocimeter \(ADV\) for turbulence measurements.](#) *Journal of Atmospheric and Oceanic Technology* **15** (1), 272–289.

First received 19 March 2020; accepted in revised form 16 June 2020. Available online 29 June 2020